

# NSCAT and QUIKSCAT Winds

## Reveal the Mysterious

### Somali Jet

David Halpern  
Jet Propulsion Laboratory  
California Institute of Technology

\*\*\*\*\*

Halpern, D., M. H. Freilich and R. A. Weller (1998) Arabian Sea surface winds and ocean transports determined from ERS-1 scatterometer. *J. Geophys. Res.*, 103, 7799-7805.

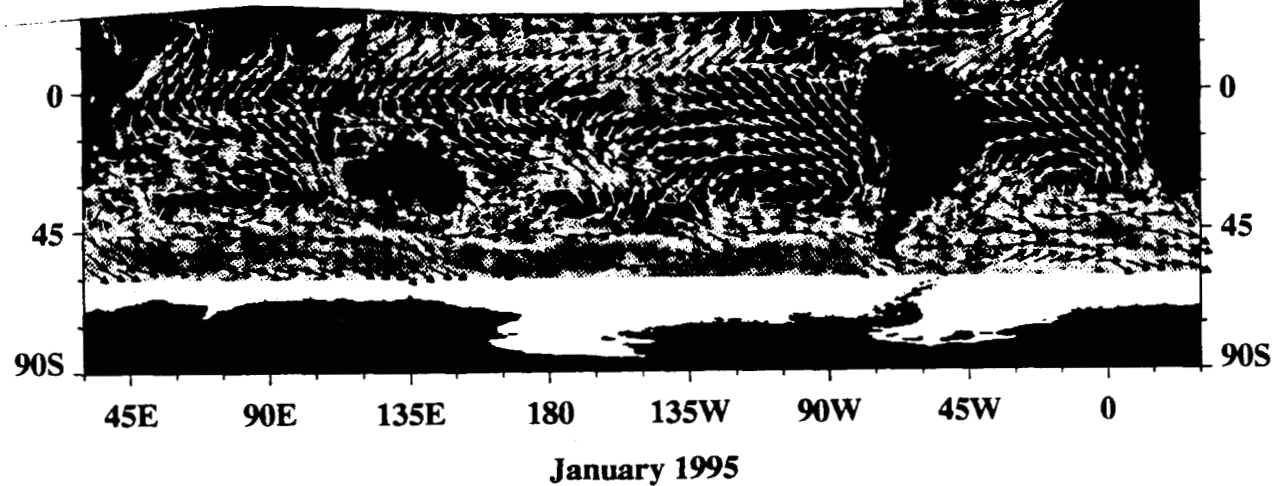
Halpern, D., M. H. Freilich and R. A. Weller (1999) ECMWF and ERS-1 surface winds over the Arabian Sea during July 1995. *J. Phys. Oceanogr.*, 29, 1619-1623.

Halpern, D. and P. M. Woiceshyn (1999) Onset of the Somali Jet in the Arabian Sea During June 1997. *J. Geophys. Res.*, 104, 18041-18046.

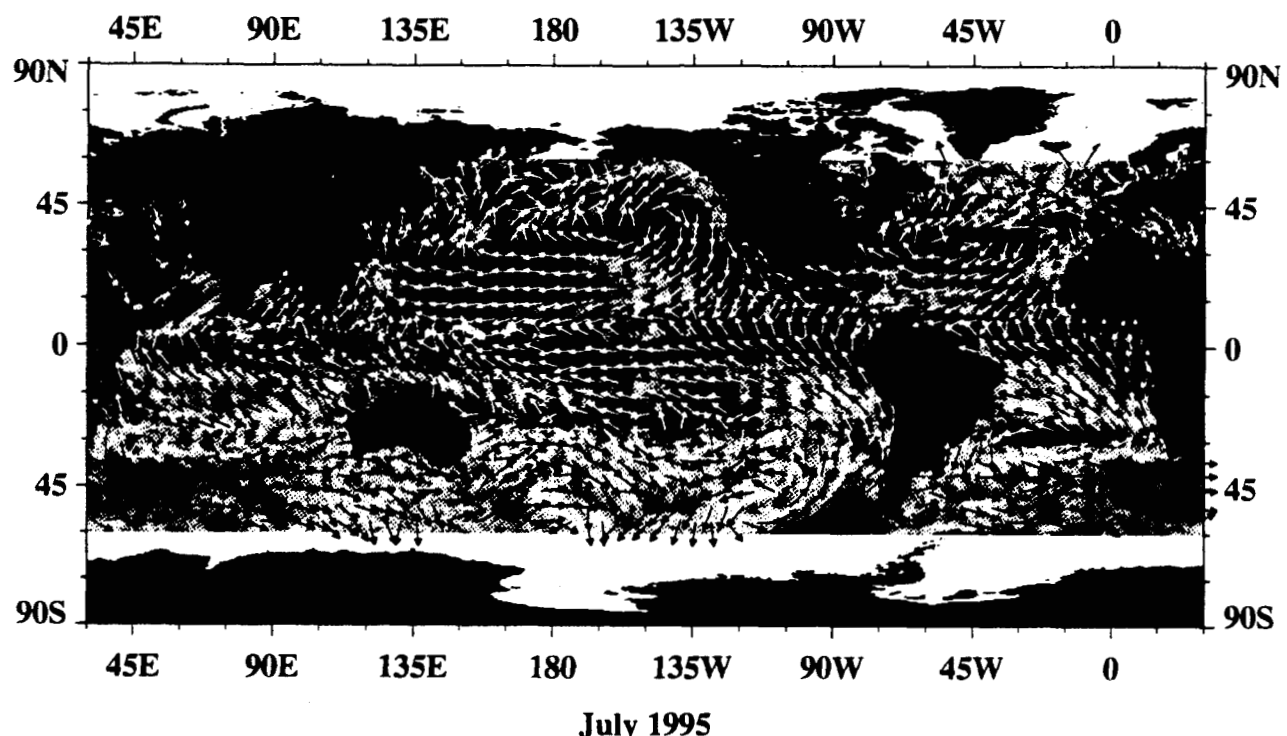
Halpern, D., V. Zlotnicki, P. Woiceshyn, O. Brown, M. Freilich and F. Wentz (1998) An atlas of monthly mean distributions of SSMI surface wind speed, AVHRR/2 sea surface temperature, AMI surface wind velocity, and TOPEX/POSEIDON sea surface height during 1995. JPL Publication 98-5, Jet Propulsion Laboratory, Pasadena, 73 pp.

In the Arabian Sea, the winds in Jan  
blow towards the southwest and are  
typical of the tropical southeast tradewinds.

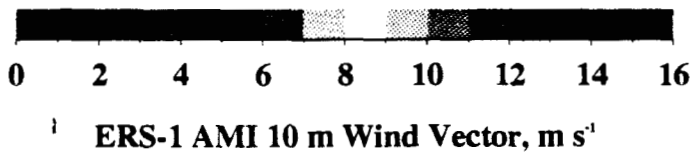
Notice the change in direction in July  
when the southwest monsoon occurs.



January 1995

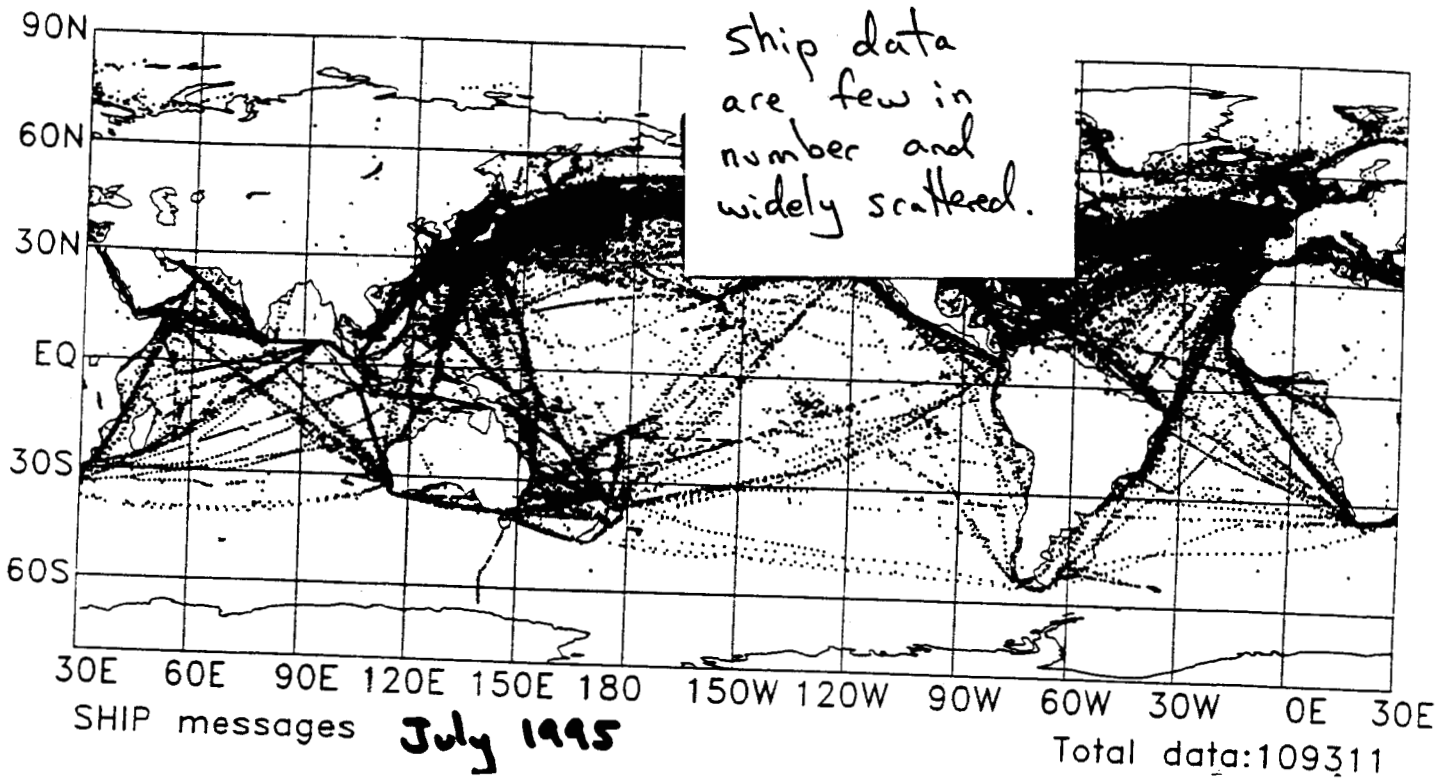


July 1995

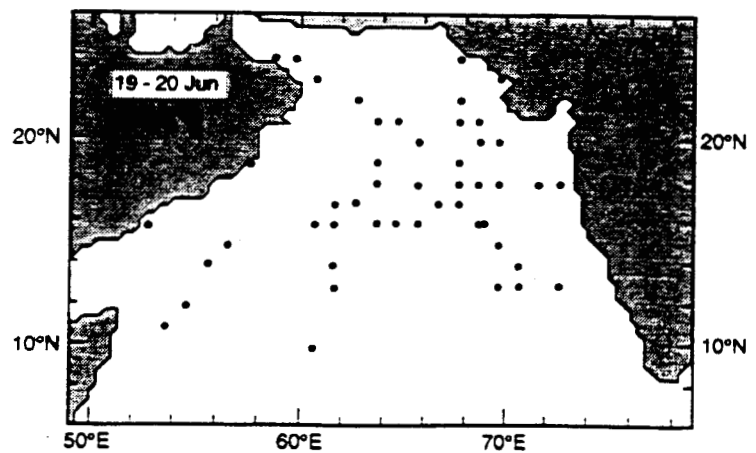
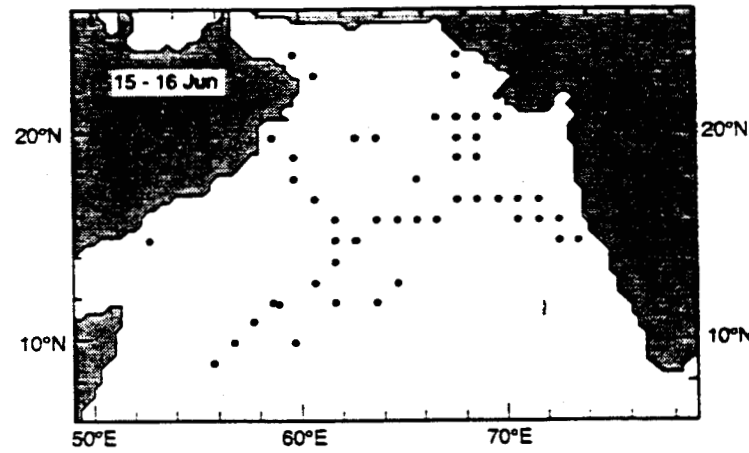
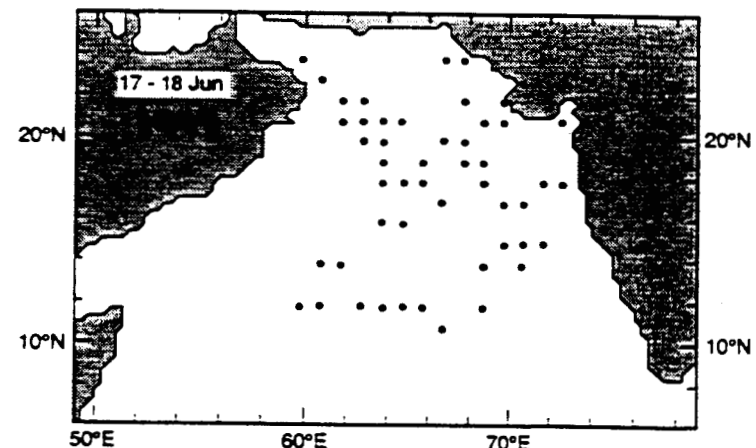
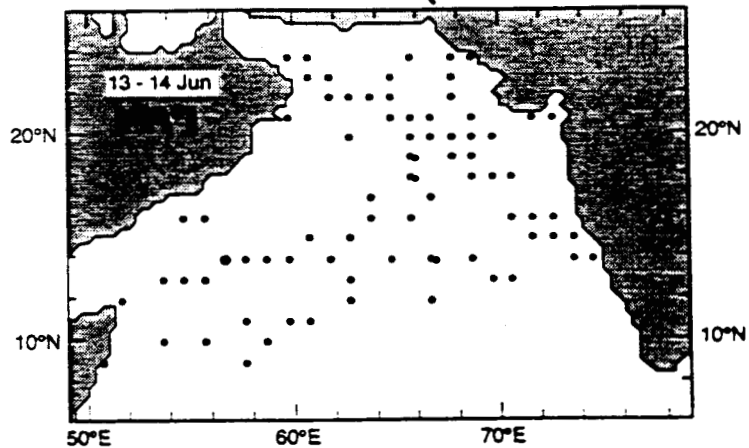


ERS-1 AMI 10 m Wind Vector, m s<sup>-1</sup>

Holpoca et al. (1998)



$1^\circ \times 1^\circ$  COADS Ship Locations



AMI on ERS  
SSMI on DMSP

under the sun



**EXPO'98**

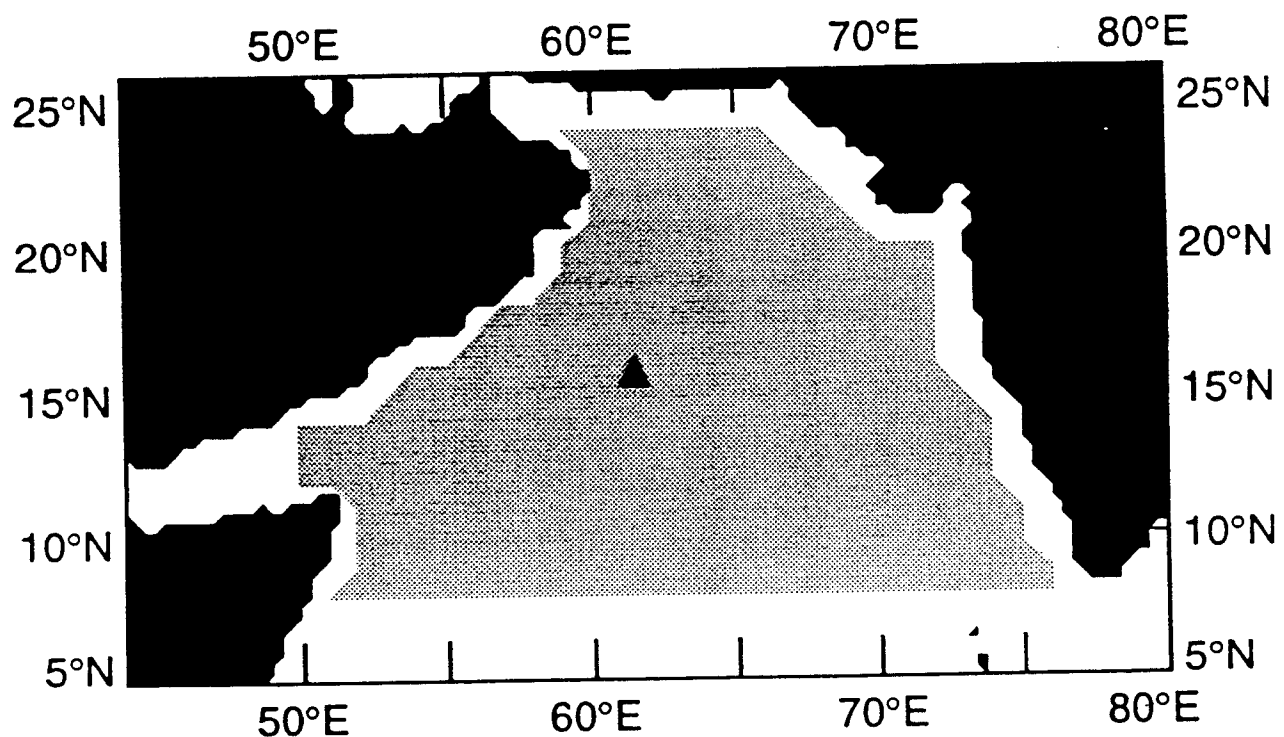


e

NASA



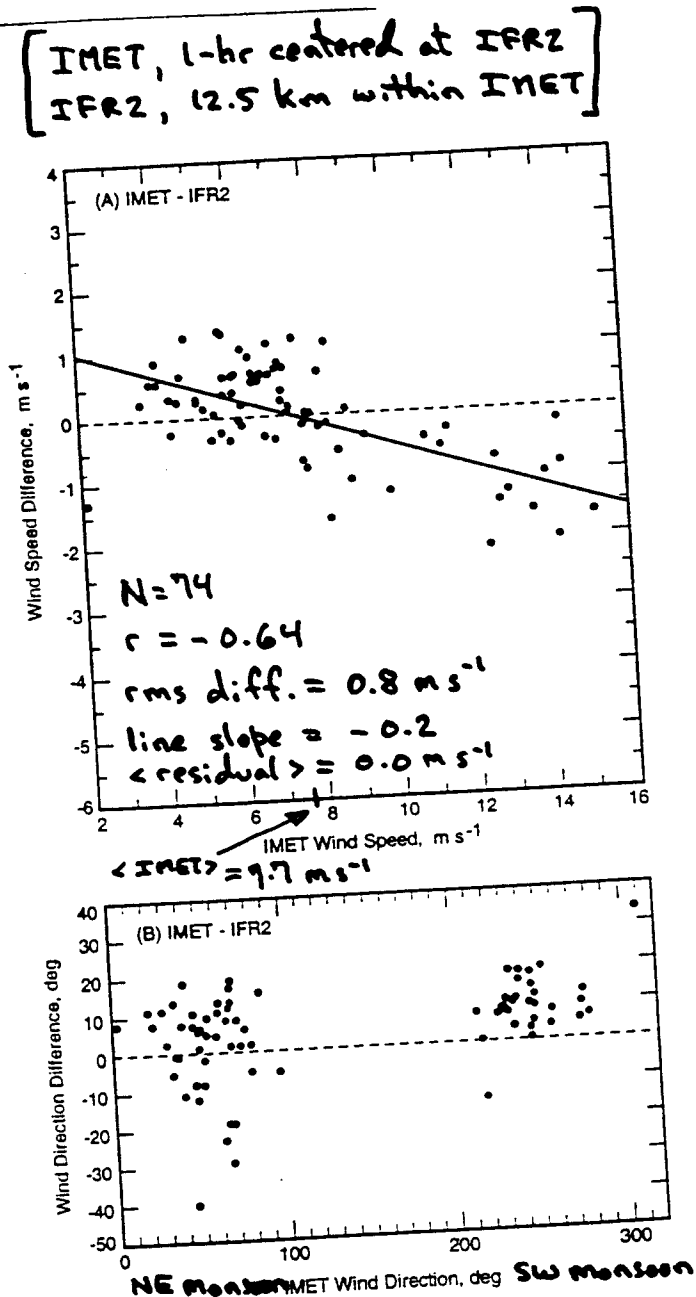
Location of the  
WHOI buoy



▲ IMET (Improved Meteorological) mooring [R. Weller, WHOI]  
Oct 1994 - Oct 1995 , redeployment in April 1995

Accuracy of  
ERS wind  
vectors

Mention FD and CMOD4



This  
side  
will  
not  
be  
shown

$$2^\circ \pm 13^\circ$$

$$n = 43$$

$$9^\circ \pm 8^\circ$$

$$n = 31$$

Halpern et al. (1998)

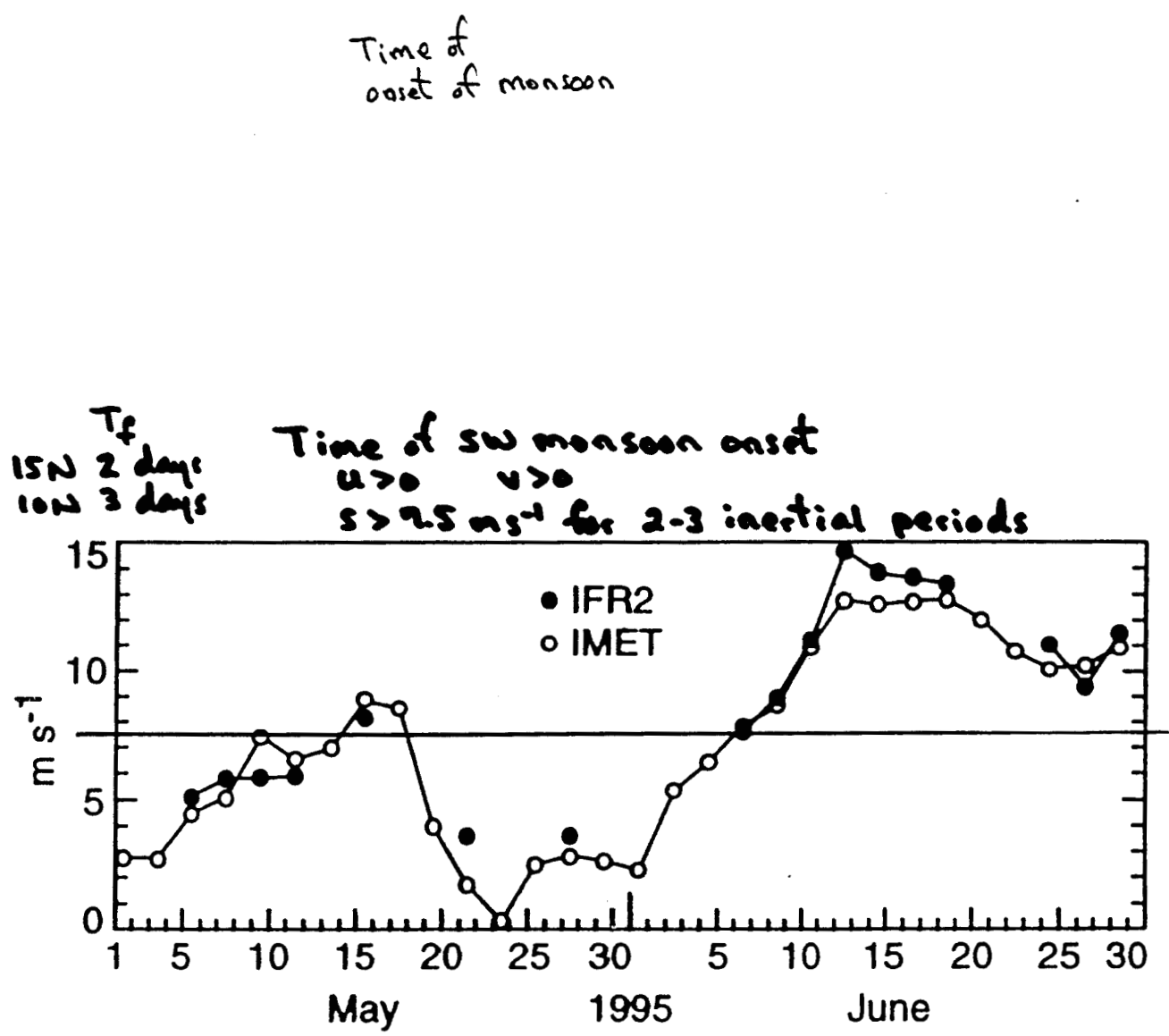
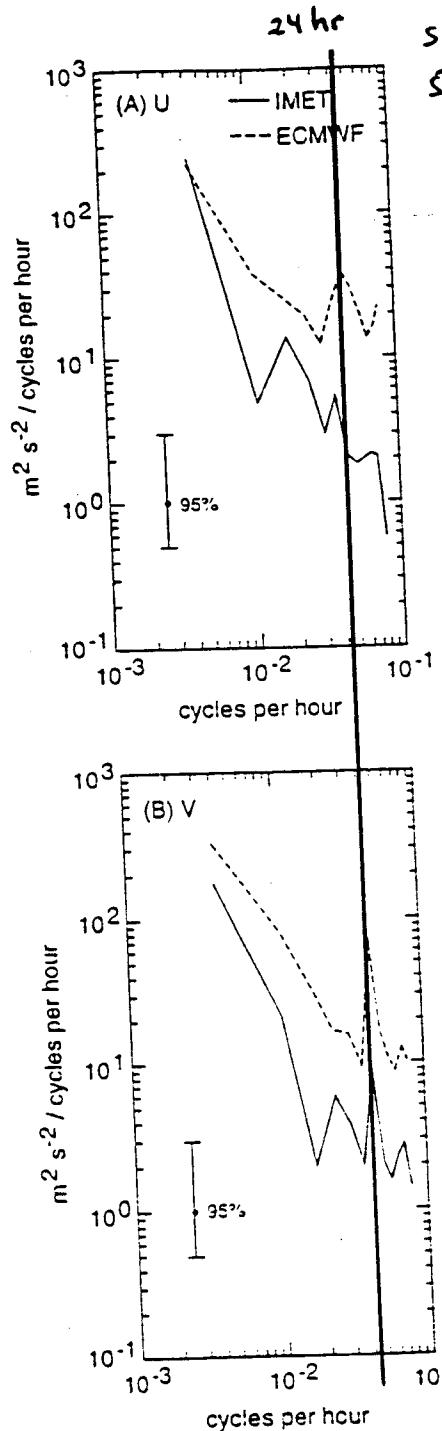


**Figure 4.** Time series of 2-day average wind speed computed from IMET (open circles) and IFR2 (solid circles) data. About 17 individual IFR2 wind vectors were averaged to form a  $1^\circ \times 1^\circ$  2-day value centered at the IMET location.

Halpern et al. (1998)



Satellite records  
small-scale  
structures.

FIG. 3. Frequency spectra of (a) east-west,  $u$ , and (b) north-south,  $v$ , wind velocity components for IMET and ECMWF data during July 1995. The 95% represents the 95% confidence levels determined from the chi-square distribution.

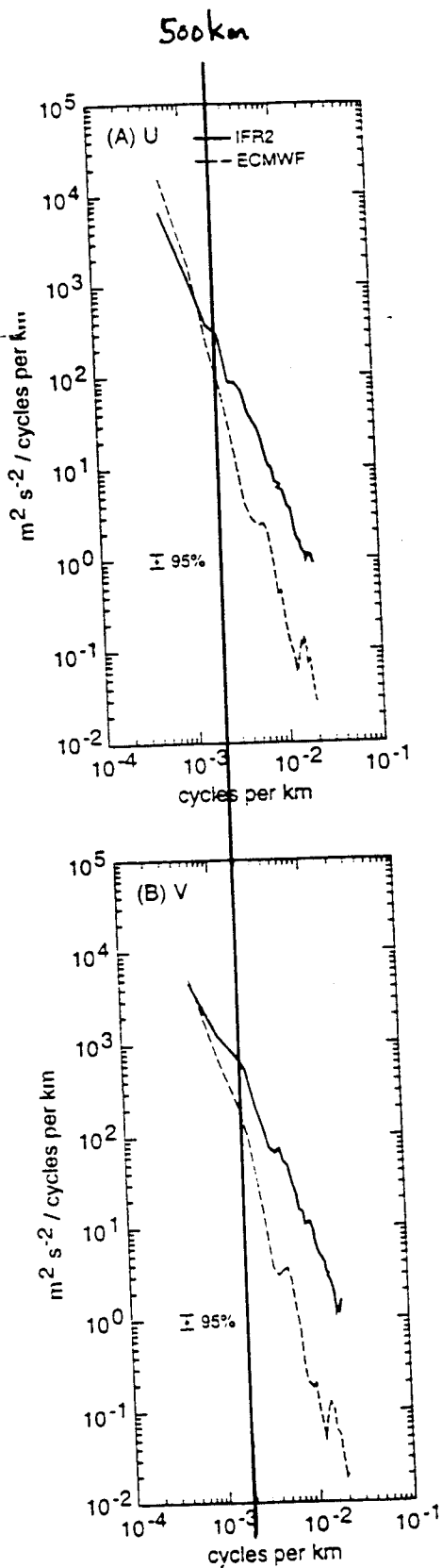


FIG. 4. Wavenumber spectra of (a) east-west,  $u$ , and (b) north-south,  $v$ , wind velocity components for ECMWF and IFR2 data during July 1995 in the central Arabian Sea. The 95% represents the 95% confidence levels determined from the chi-square distribution.

# Wind-Driven Ocean Transports

$$\left[ \text{curl}_z \tau^* = \frac{\partial \tau_y^*}{\partial x} - \frac{\partial \tau_x^*}{\partial y}, \quad f = 2\Omega \sin \theta, \quad \beta = \frac{2\Omega \cos \theta}{R} \right]$$

- vertical

$$\iint_{x,y} \left( \frac{1}{\rho f} \right) \left( \text{curl}_z \tau^* + \beta \frac{\tau_x^*}{f} \right) dx dy$$

- $y$ -component Ekman

$$\int_x -\frac{\tau_x^*}{\rho f} dx$$

- Sverdrup

$$\int_x \left( \frac{\text{curl}_z \tau^*}{\rho \beta} \right) dx$$



$$1 \text{ Sv} = 1 \times 10^6 \text{ m}^3 \text{ s}^{-1}$$

[Gulf Stream transport  $\sim 100 \text{ Sv}$ ]

[River transport  $\sim 1 \text{ Sv}$ ]

Rain, freshwater transfer  
= 10 Sv

The vertical velocity at the bottom of the Ekman layer associated with divergence and convergence in the Ekman layer is

$$W_E = \frac{1}{\rho f} [\text{curl}_z \tau - \beta M_y^E]$$

$$\rho = 1025 \text{ kg m}^{-3}$$

$$f = 2 \Omega \sin \theta$$

$$\beta = \frac{df}{dy} = \frac{2 \Omega \cos \theta}{R}$$

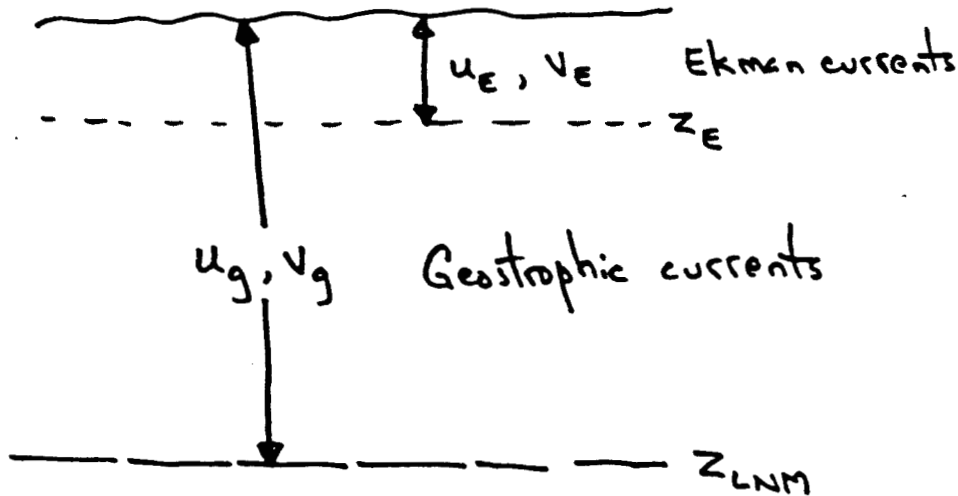
$M_y^E$  = Ekman mass transport (per unit width)  
in  $y$ -direction =  $-\frac{\tau_x}{f}$

$$\text{curl}_z \tau = \frac{\partial \tau_y}{\partial x} - \frac{\partial \tau_x}{\partial y}$$

$$(\tau_x, \tau_y) = \rho_a C_s (u, v) (u^2 + v^2)^{1/2}$$

$$\rho_a = 1.225 \text{ kg m}^{-3}$$

# Sverdrup Transport



$$u = u_E + u_g$$

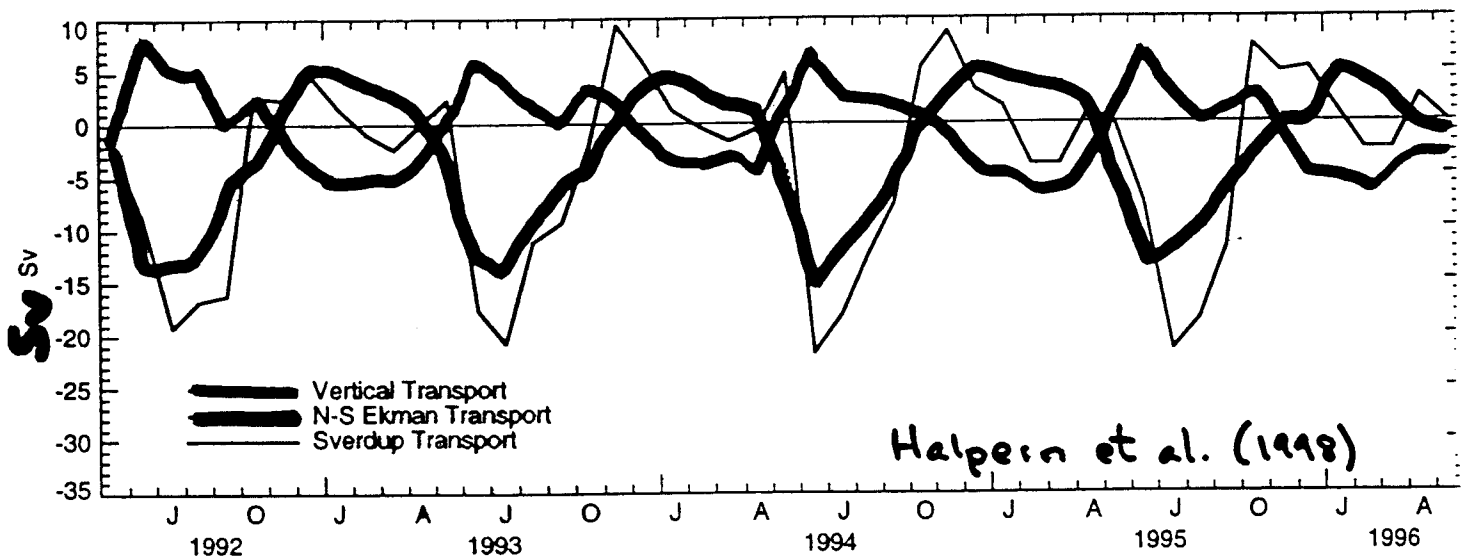
$$v = v_E + v_g$$

$$M_y = \int_{z_{LNM}}^{z=0} \rho v dz$$

$$M_y = \frac{\text{curl}_z T^*}{\beta}$$

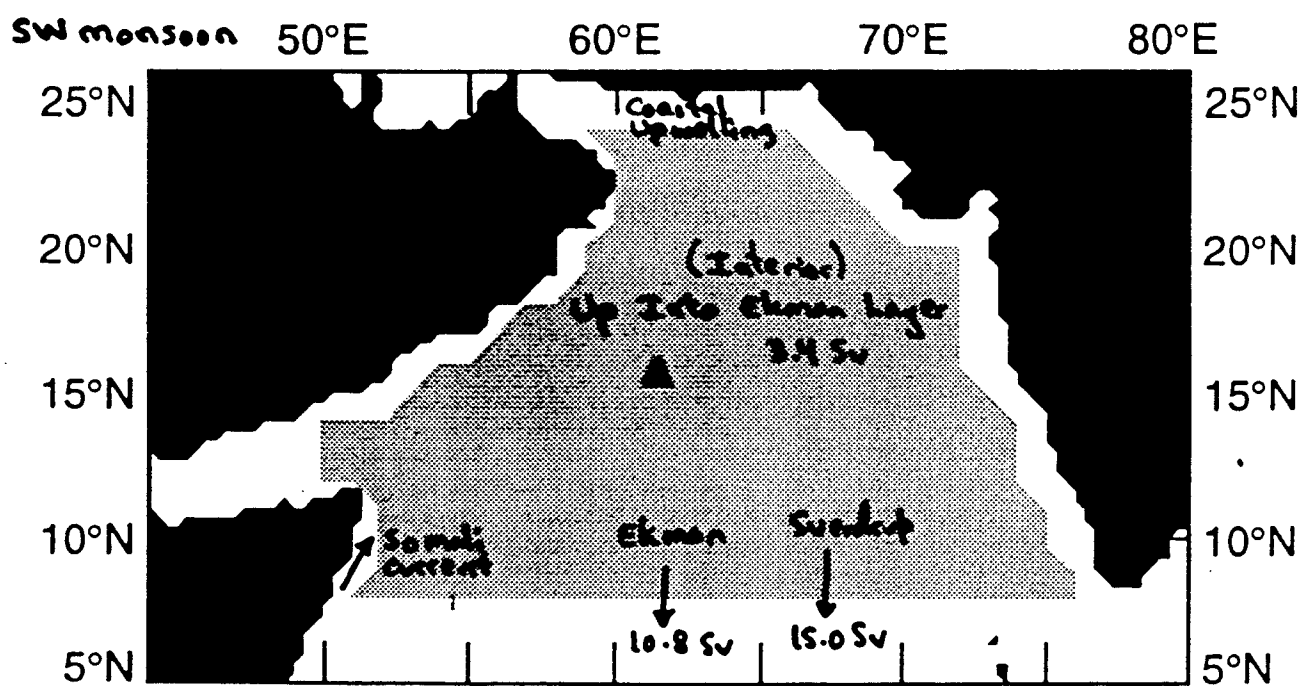
Sverdrup transport  
per unit zonal width  
[integrated north-south  
current from  $z=0 \rightarrow z_{LNM}$ ]

$$\text{Sverdrup Transport} = \int_x M_y dx$$

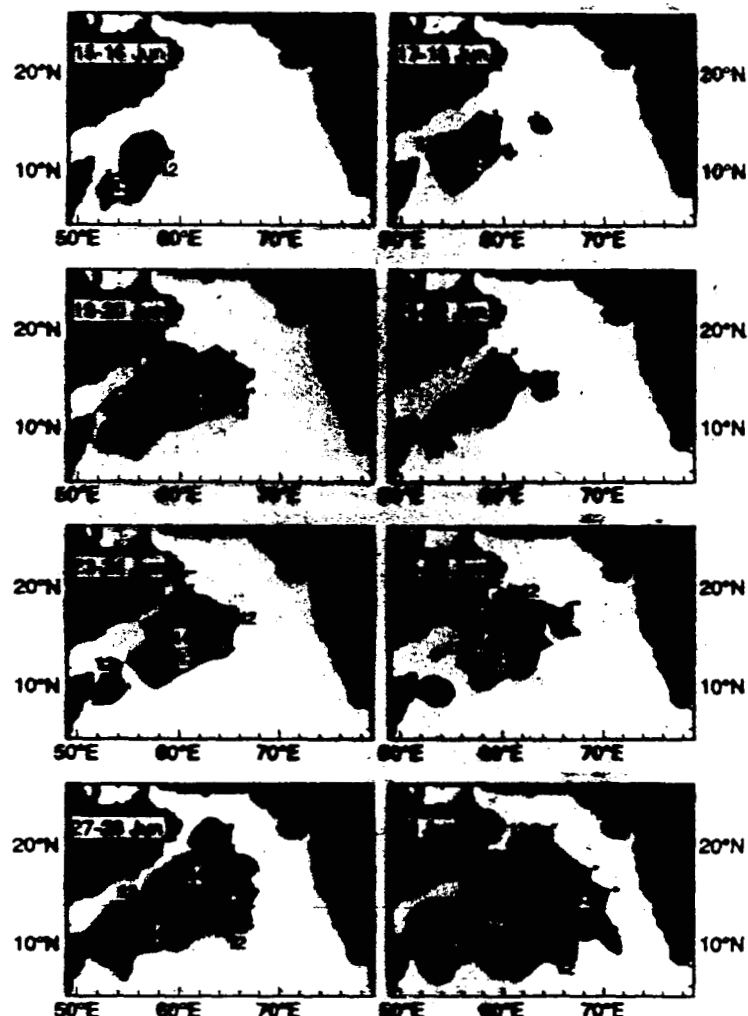


Halpern et al. (1998)

	SW Monsoon	NE Monsoon
	4-year Mean	4-year Mean
Vertical	-0.5	3.4
N-S Ekman	-2.7	-10.8
Sverdrup	-4.0	-15.0



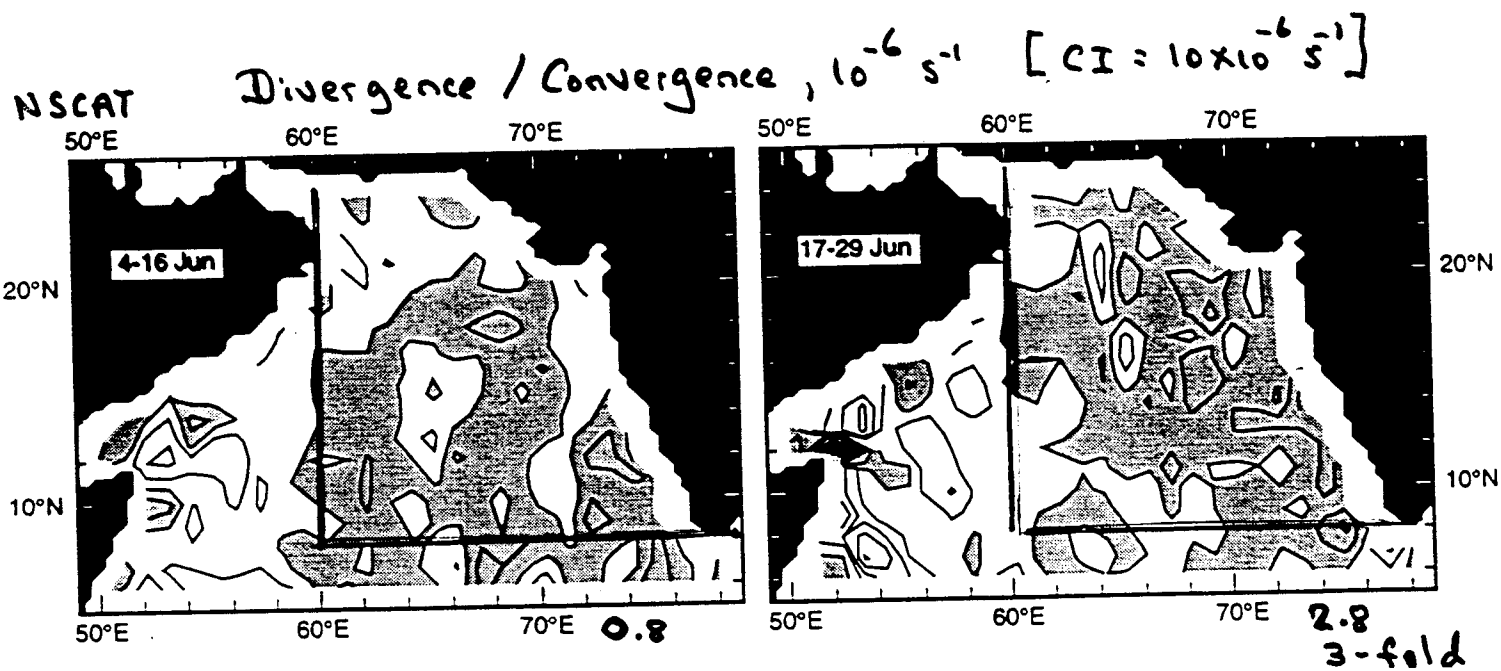
## NSCAT Provides First Look at Somali Jet Pulsation



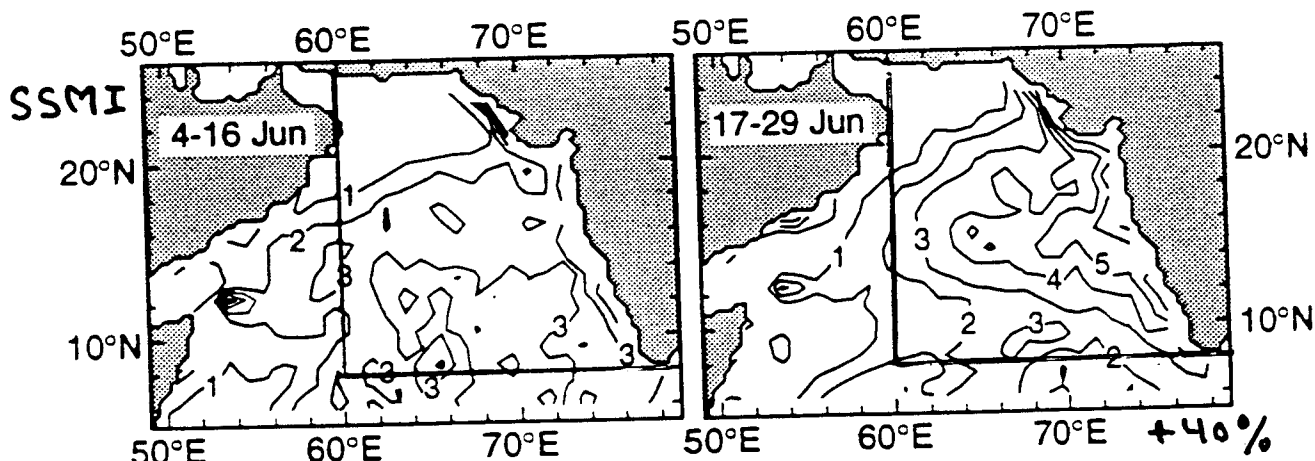
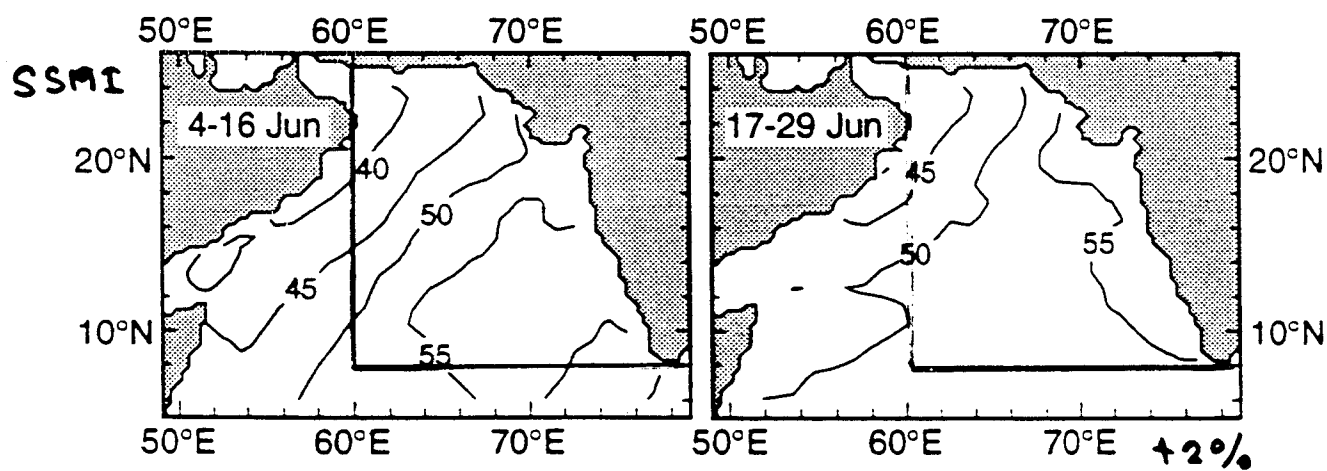
Pulsations of the Somali Jet, which is the intense southwesterly surface winds over the Arabian Sea, were undetected over the Arabian Sea until the launch of NSCAT because of insufficient simultaneous wind vector observations.

The diagram shows the eastward expansion of Somali Jet high winds ( $> 12 \text{ m s}^{-1}$ ) at 2-day intervals. The initial onset of high winds preceded by 3-4 days the time of onset of rainfall in Goa, which is on the west coast of India at about  $15^\circ\text{N}$ . Associated with the eastward advance of the Somali Jet were substantial increases in NSCAT-derived surface wind convergence and SSMI-derived integrated cloud liquid water content. Additional studies are necessary to show that Goa rainfall was related to the eastward propagating Somali Jet.

Halpern, D. and P. Woiceshyn, Onset of the Somali Jet in the Arabian Sea During June 1997. *Journal of Geophysical Research*, 104, [1], 1999.

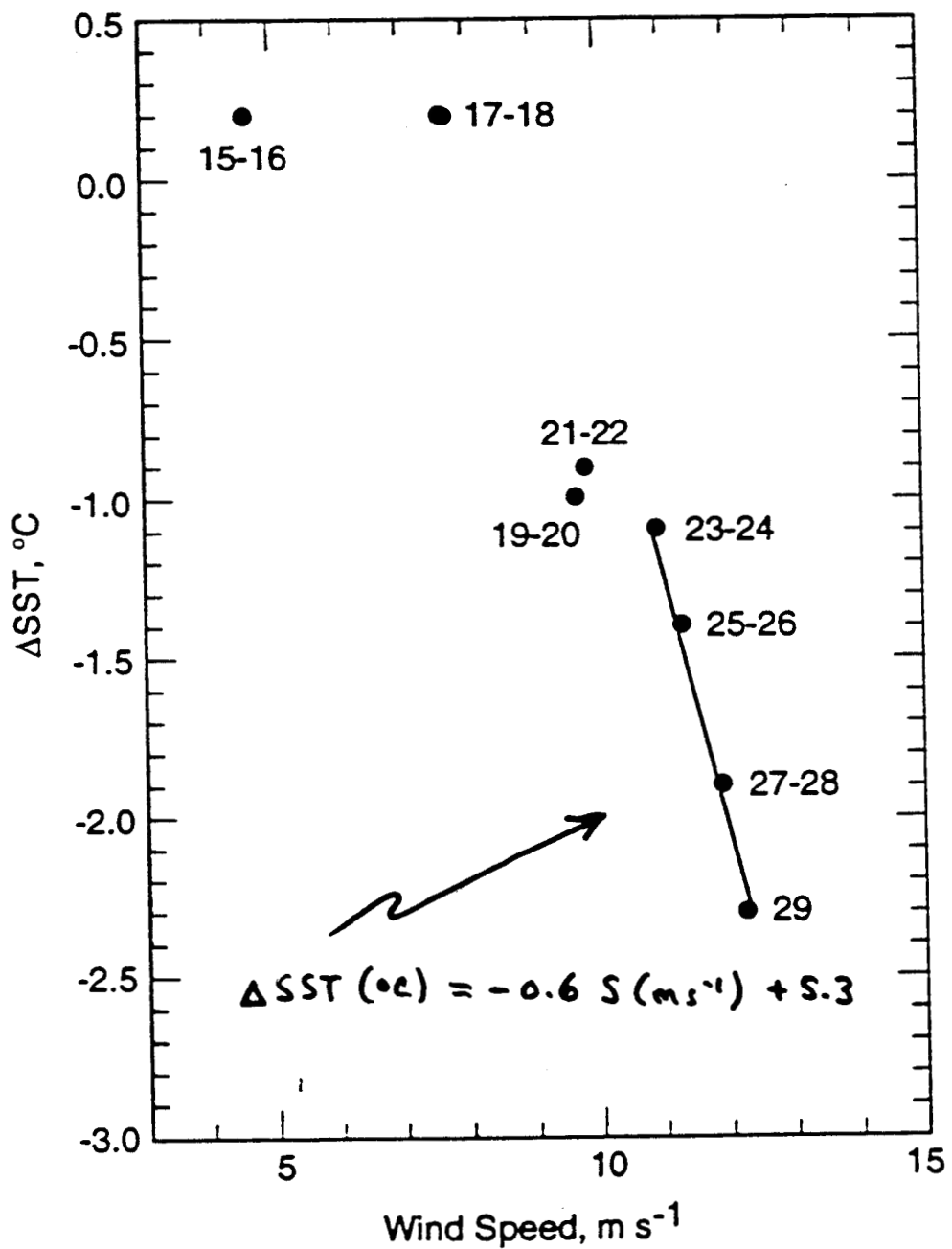
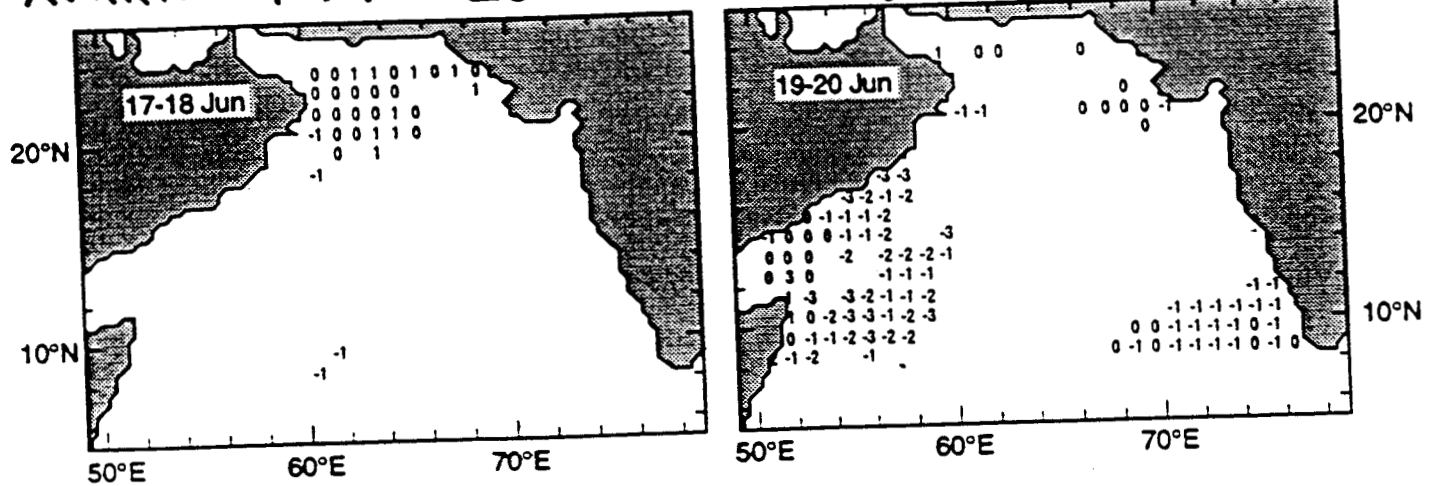


Integrated Water Vapor (Total Precipitable Water), mm

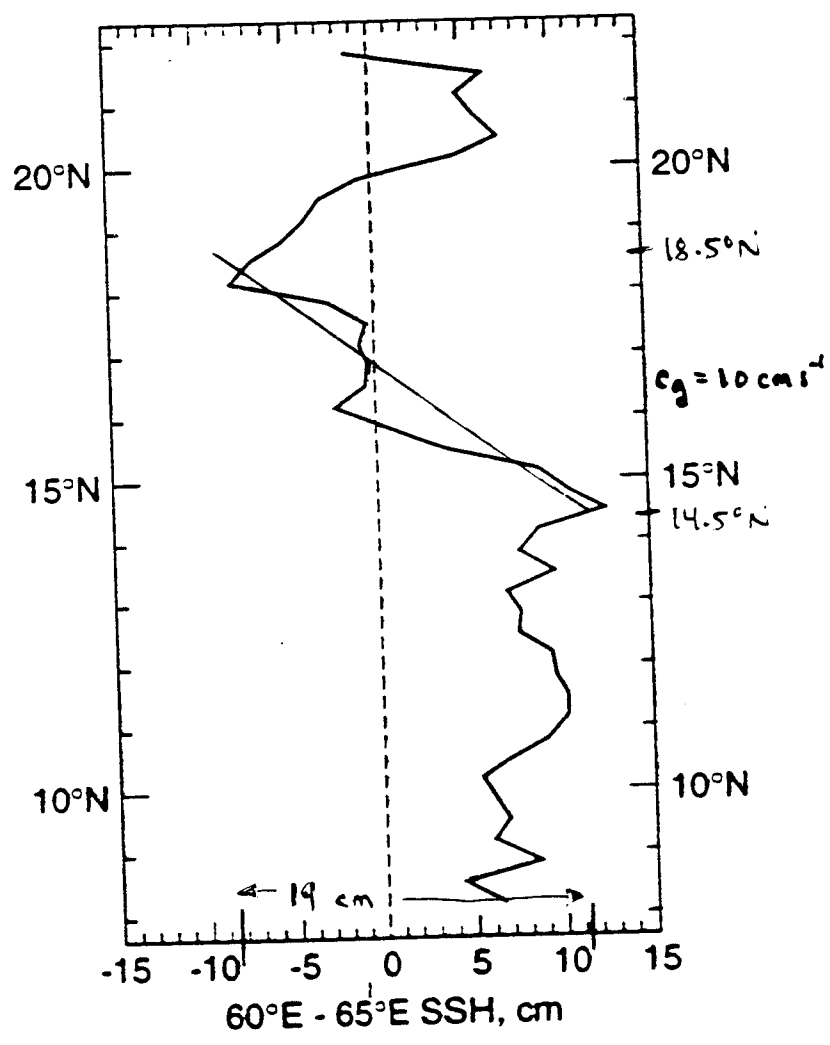
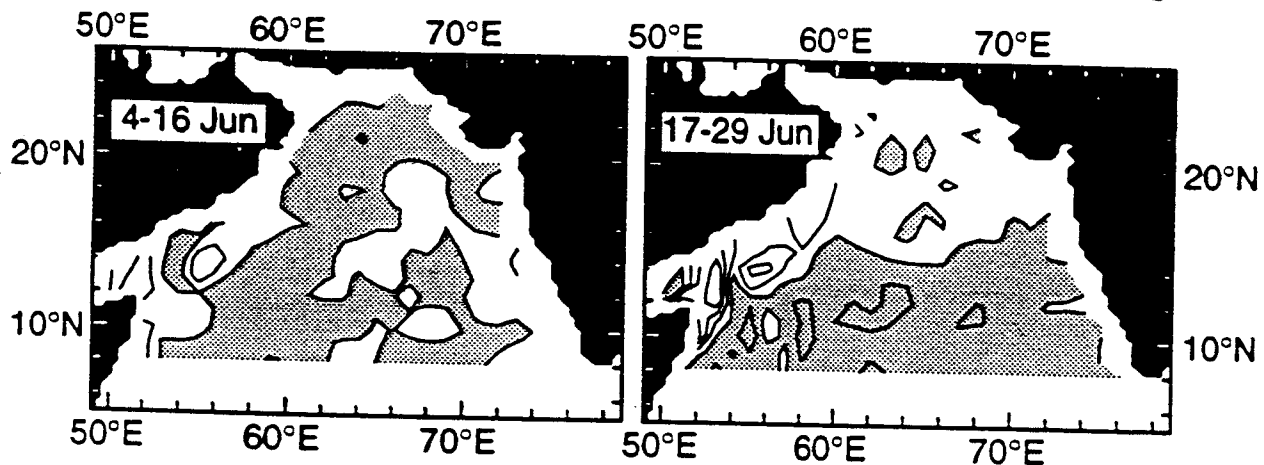


Integrated Cloud Liquid Water Content (0.1mm)

AVHRR  $1^\circ \times 1^\circ$   $\Delta SST = SST_{2\text{-day}} - SST_{1-14\text{ Jun}}$   ${}^\circ\text{C}$

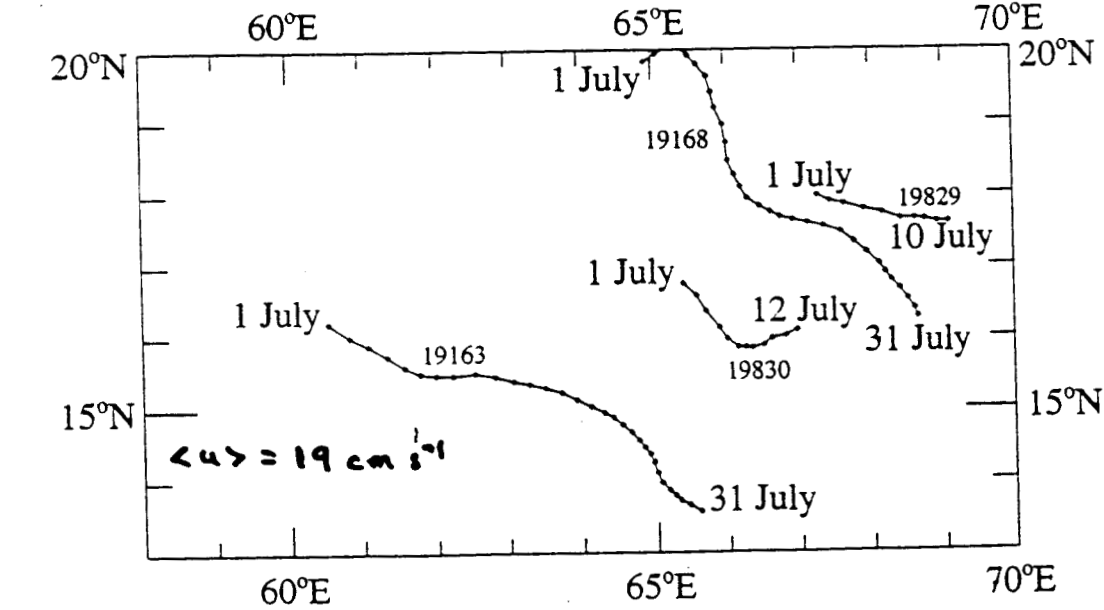
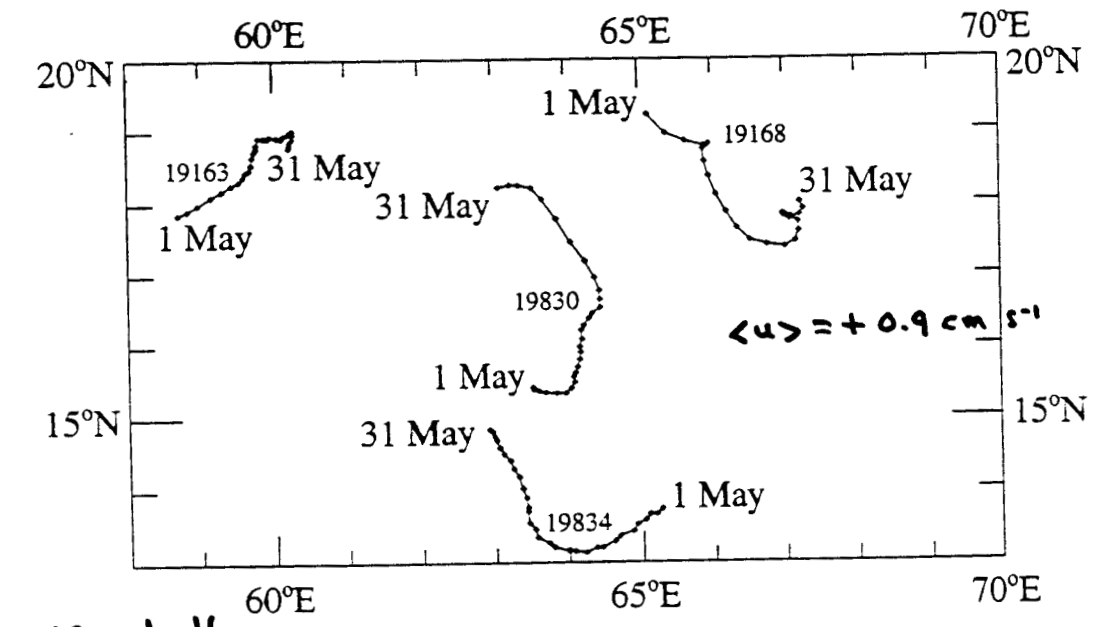
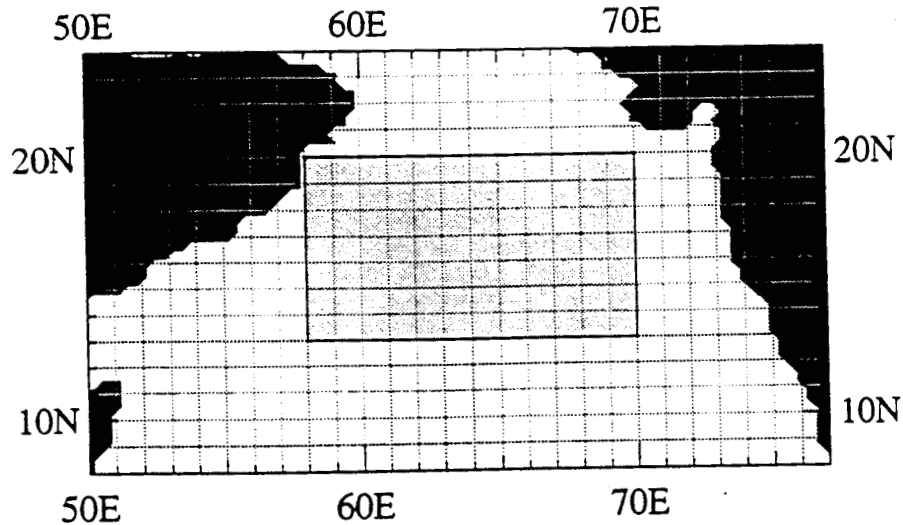


$W_E, 10^{-6} \text{ m s}^{-1}$  [ $\text{CI} = 10 \times 10^{-6} \text{ m s}^{-1}$ ]

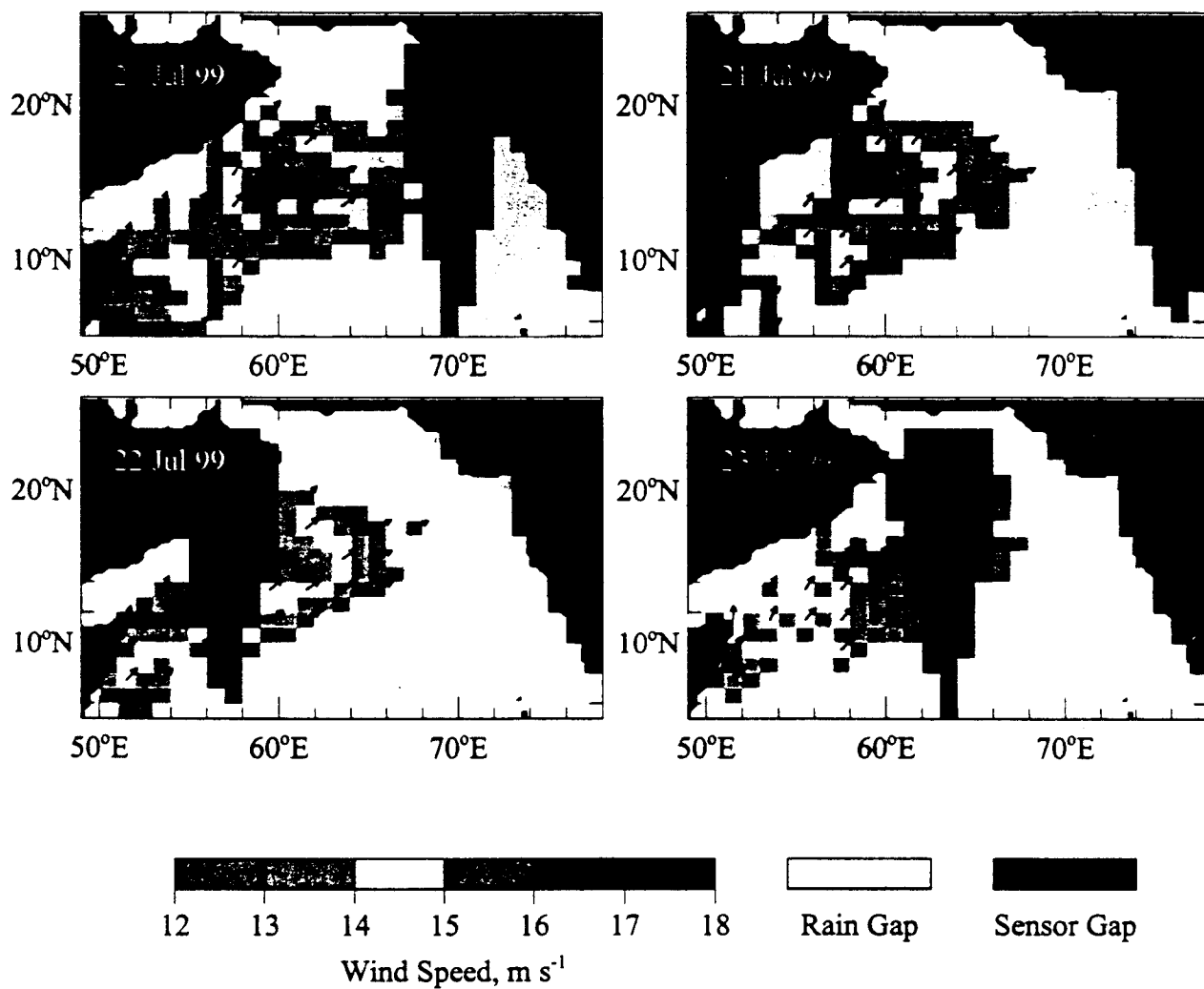


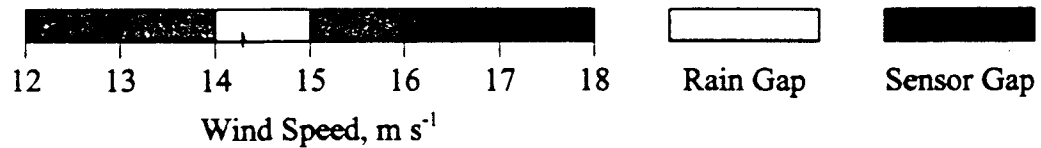
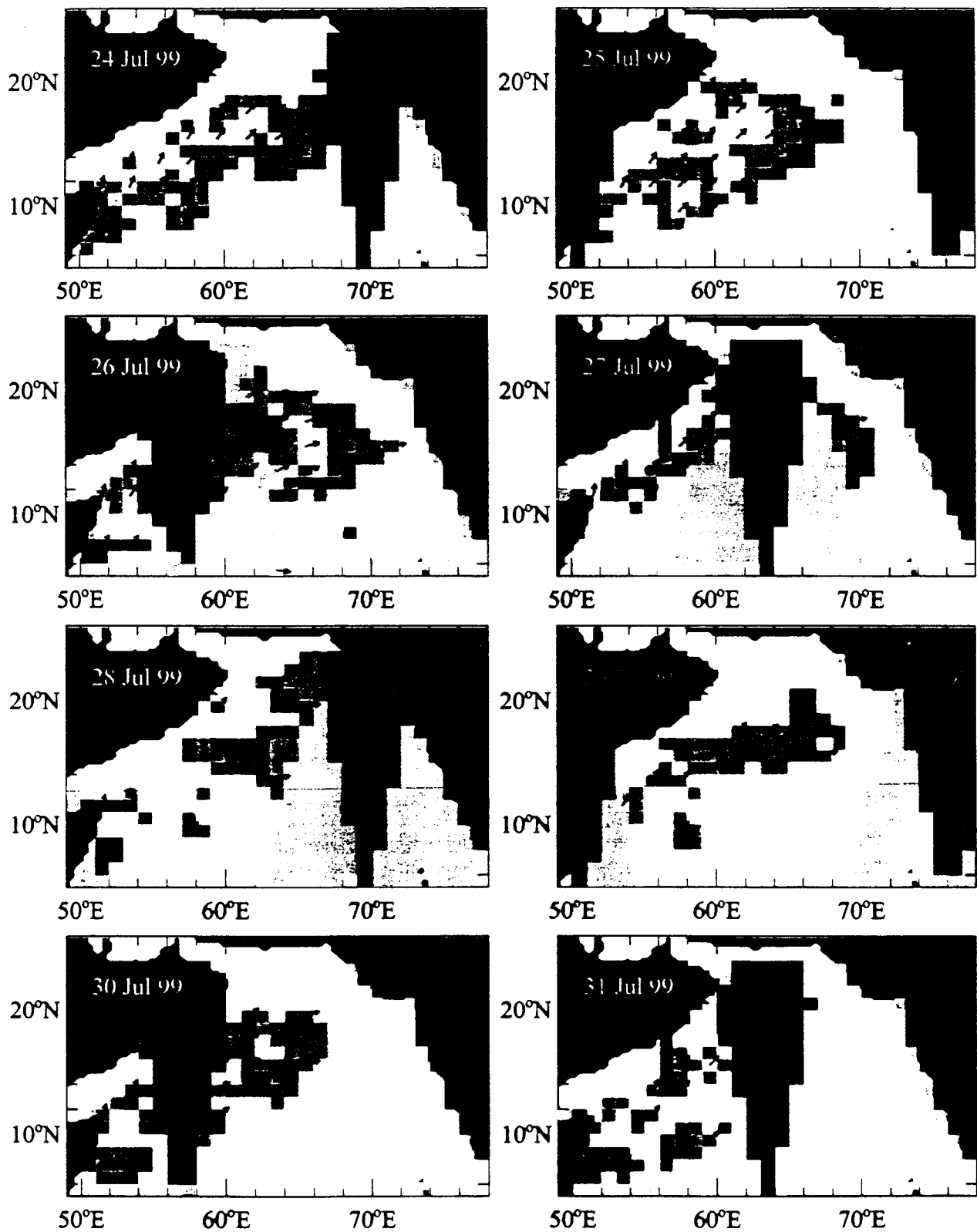
July - minus - May 1997

## Daily Buoy Locations in May and July 1997



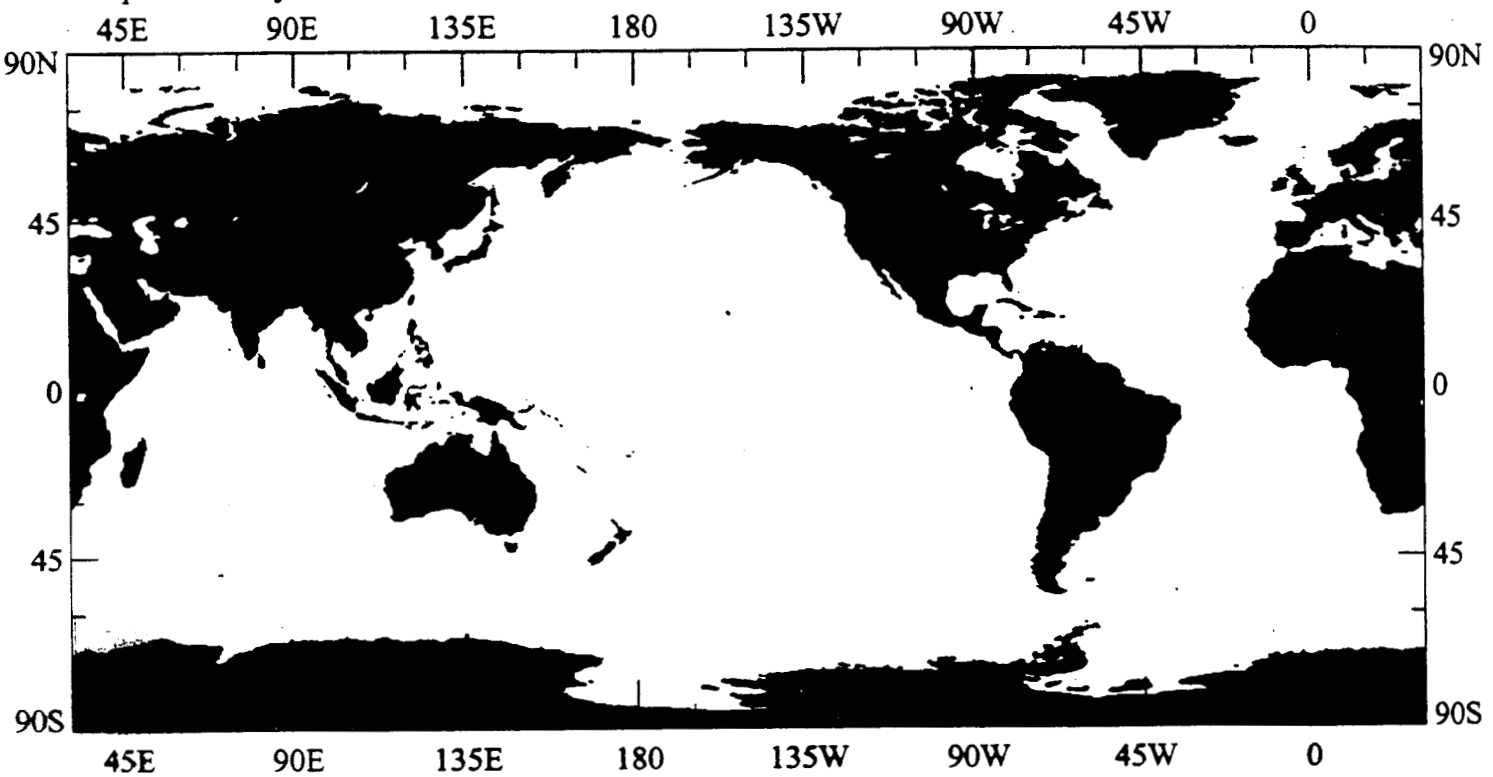
QuikScat  
not contaminated by rain





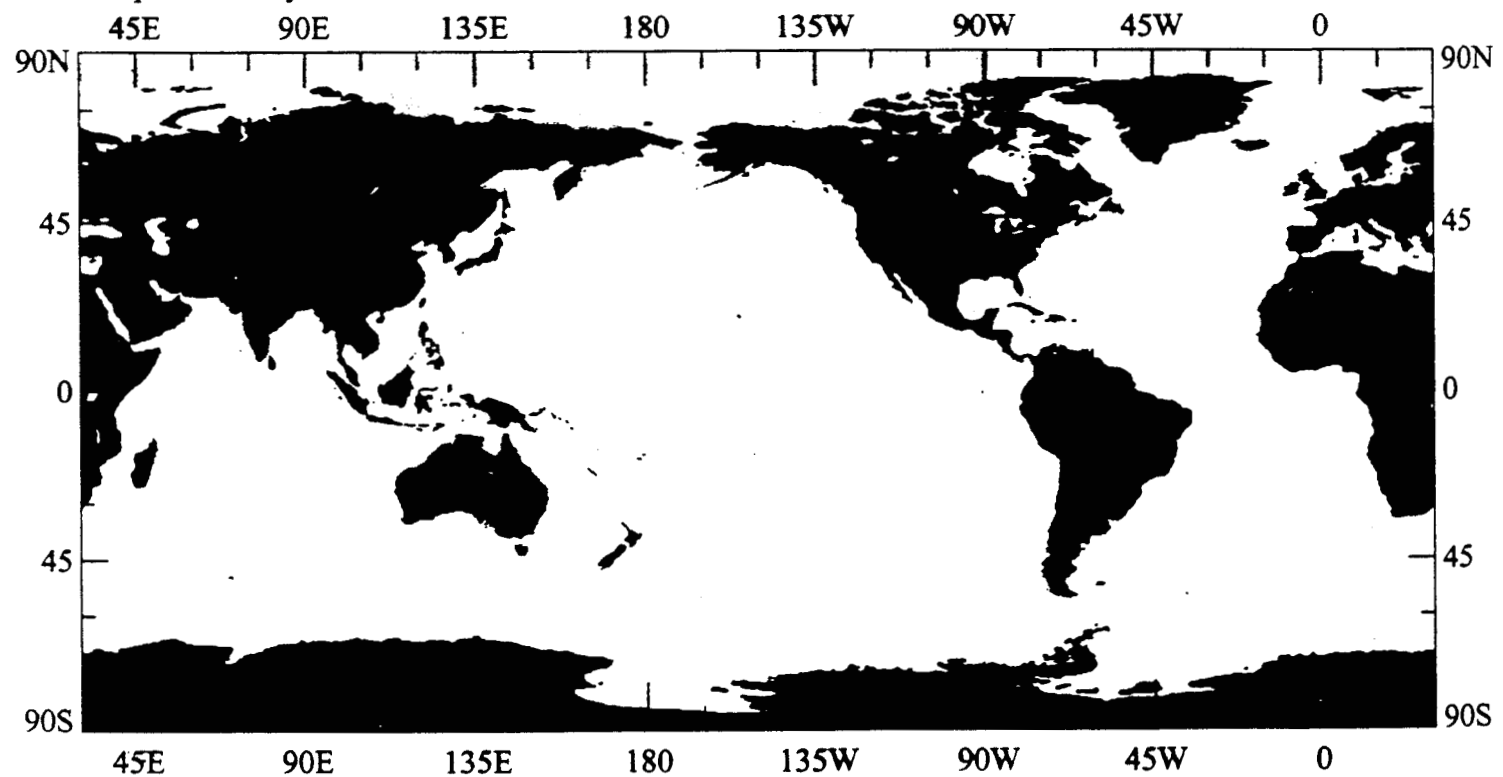
26 October 1999 - QuikScat (prelim) -  $1^{\circ} \times 1^{\circ}$  (Y.M.)

Data Gaps Shown by Green Areas



27 October 1999 - QuikScat (prelim) -  $1^{\circ} \times 1^{\circ}$  (Y.M.)

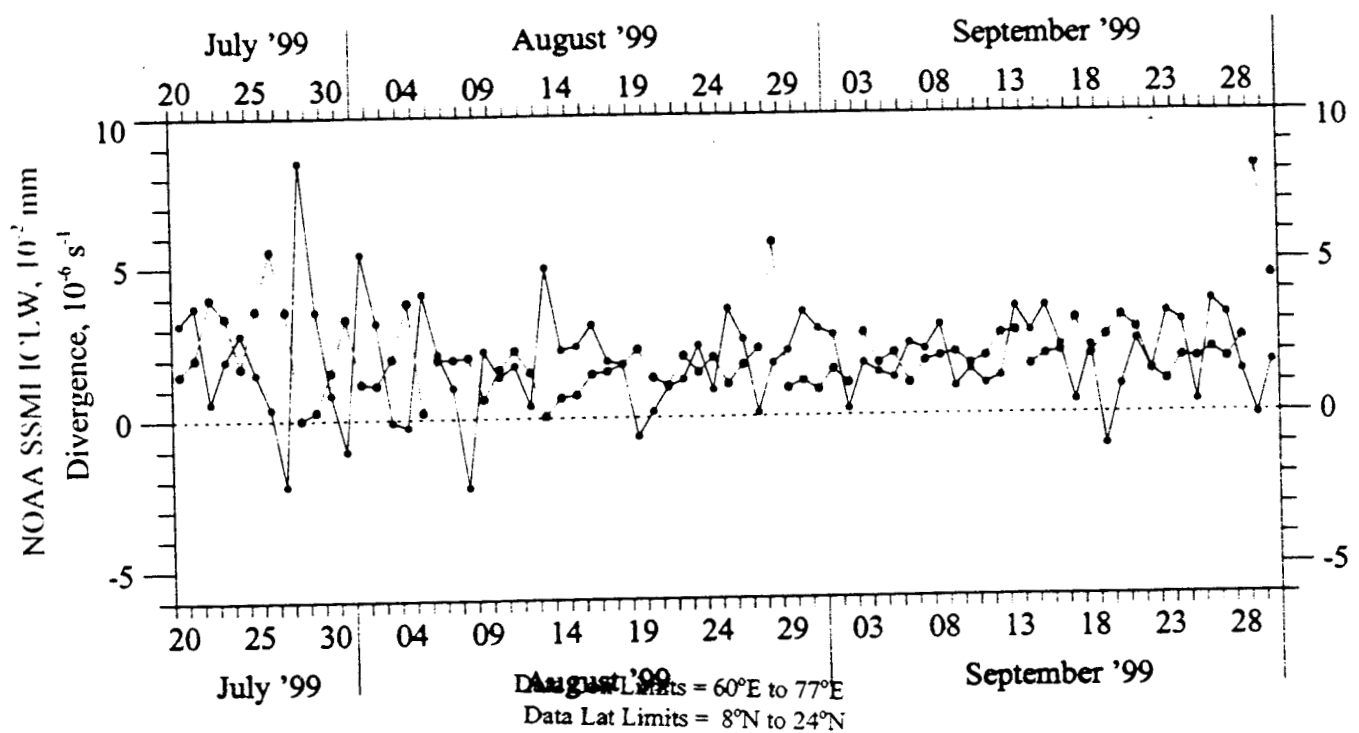
Data Gaps Shown by Green Areas



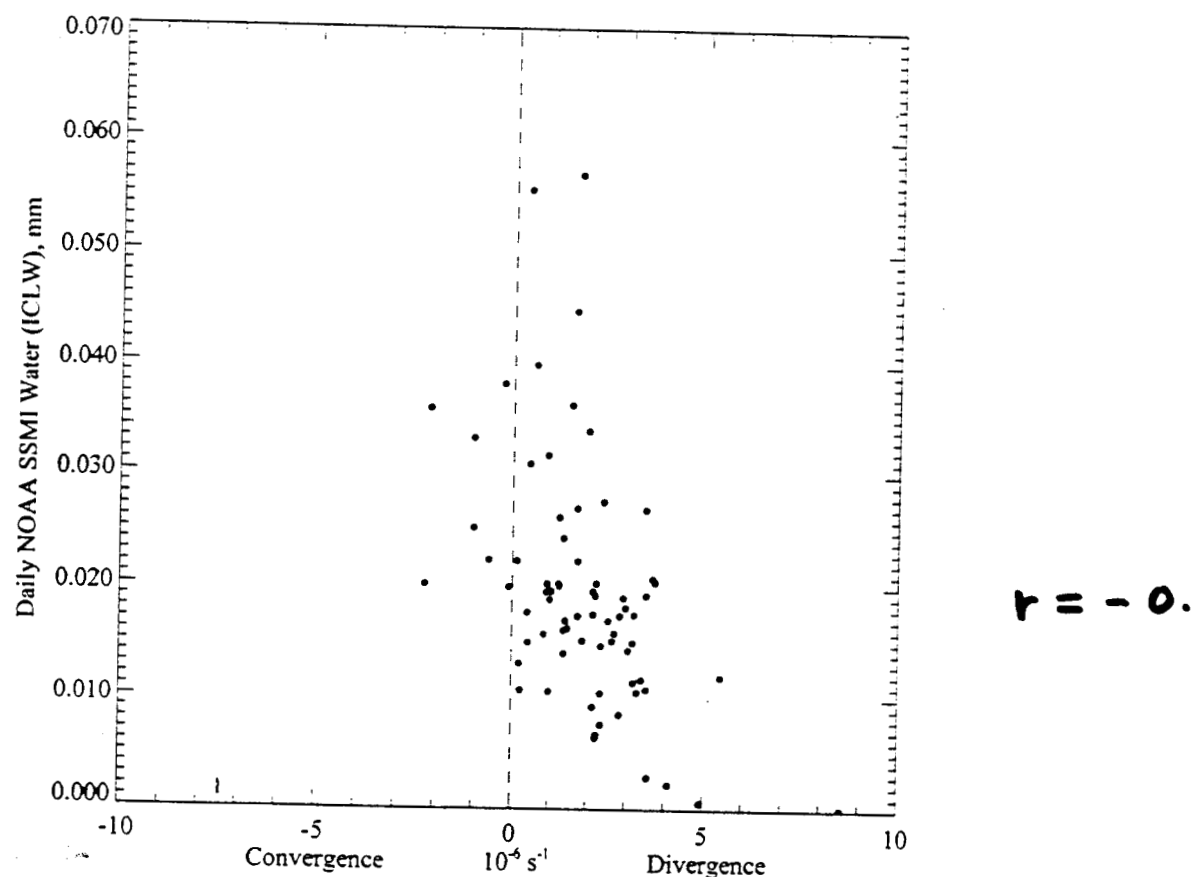
8°N - 24°N, 60°E - 77°E

Mean Daily NOAA SSMI ICLW at QuikScat/Prelim Data Locations (RED)

Daily QuikScat/Prelim (Not Contaminated by Rain) Mean Divergence (BLUE)



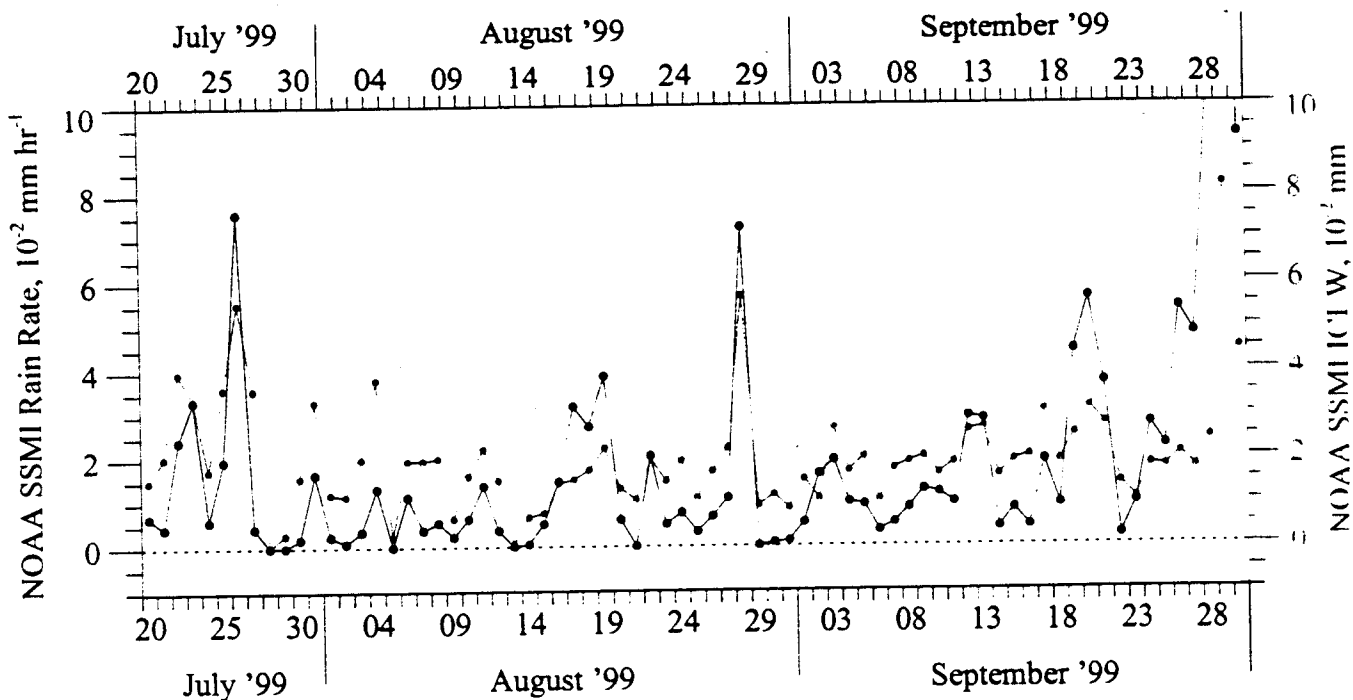
August Limits = 60°E to 77°E  
Data Lat Limits = 8°N to 24°N



8°N - 24°N, 60.5°E - 77°E

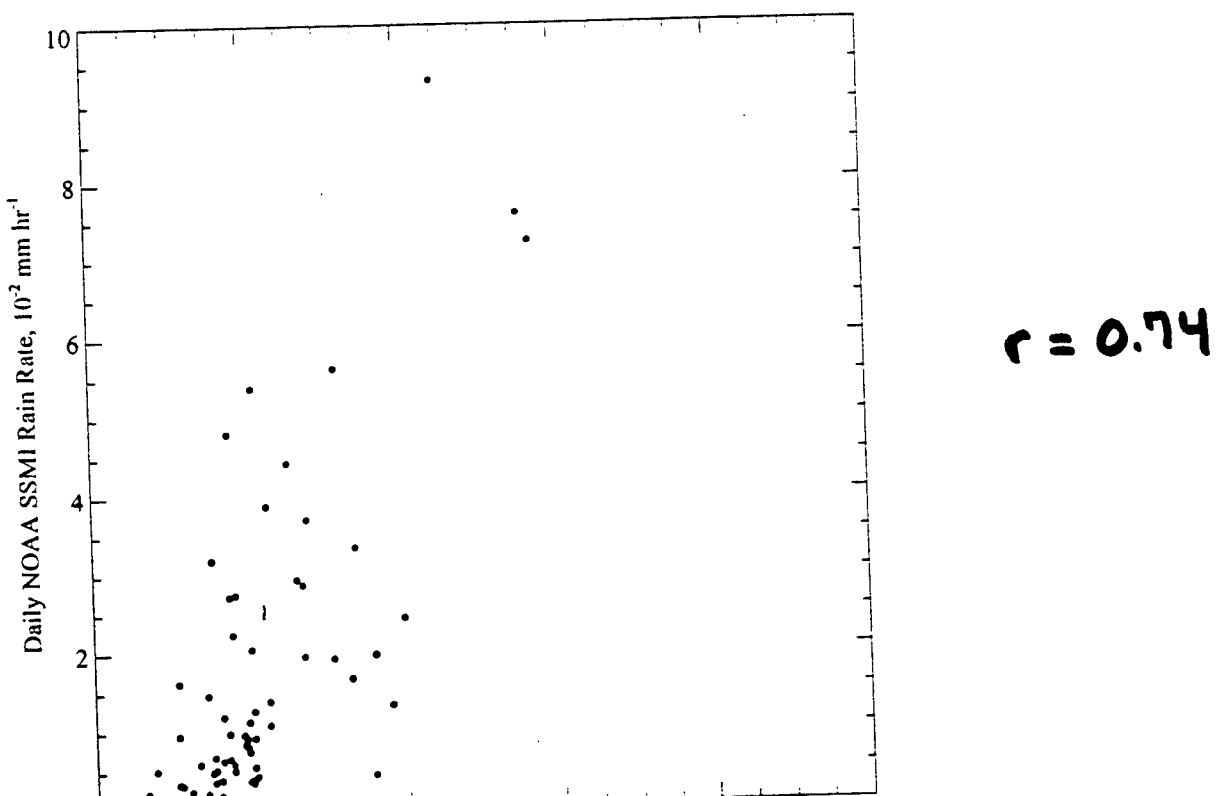
Mean Daily NOAA SSMI Rain at QuikScat/Prelim Divergence Data Locations (BLUE)

Mean Daily NOAA SSMI ICLW at QuikScat/Prelim Divergence Data Locations (RED)



Data Lon Limits = 60.5°E to 77°E

Data Lat Limits = 8°N to 24°N



# SUMMARY

Eastern Arabian Sea

$$\nabla_H \cdot \vec{u} \downarrow_{\text{conv}}^{\text{div}}$$

IWV  $\uparrow\downarrow$  no change

ICLW  $\uparrow$

RainRate  $\uparrow$